Innovative Hydroxyapatite/Bioactive glass composites processed by spark plasma sintering for bone tissue repair

Devis Bellucci[1*], Luca Desogus[2], Selena Montinaro[2], Roberto Orrù[2], Giacomo Cao[2], Valeria Cannillo[1]

[1]*Dipartimento di Ingegneria Enzo Ferrari, Unità di Ricerca del Consorzio Interuniversitario Nazionale per la Scienza e Tecnologia dei Materiali (INSTM) - Università degli Studi di Modena e Reggio Emilia, Via P. Vivarelli 10, 41125 Modena, Italy*

[2]*Dipartimento di Ingegneria Meccanica, Chimica e dei Materiali, Unità di Ricerca del Consorzio Interuniversitario Nazionale per la Scienza e Tecnologia dei Materiali (INSTM) - Università degli Studi di Cagliari, via Marengo 2, 09123 Cagliari, Italy*

[*] Corresponding-Author: Dr. D. Bellucci

Dipartimento di Ingegneria Enzo Ferrari, Unità di Ricerca del Consorzio Interuniversitario Nazionale per la Scienza e Tecnologia dei Materiali (INSTM) - Università degli Studi di Modena e Reggio Emilia, Via P. Vivarelli 10, 41125 Modena, Italy

Telephone: +39-059-2056233; fax: +39-059-2056243; e-mail: devis.bellucci@unimore.it

Abstract

Hydroxyapatite-based composites (HA-C) with bioglass as second phase are usually produced by hot-pressing or pressureless sintering. However, using such methods

thermal levels which exceed the crystallization temperature of the glass are generally required, with possible negative effects on the bioactivity of the final system. Spark plasma sintering (SPS) is a powerful consolidation technique in terms of both processing time and temperature. In this work SPS has been employed, for the first time, to obtain HA-C with an innovative bioglass as second phase. Such glass was specifically designed to be used whenever a thermal treatment is required, thanks to its low tendency to crystallize. A systematic study is conducted in order to identify the optimal sintering conditions for preparing highly dense composites and, at the same time, to minimize the crystallization of the glassy phase. The obtained samples are highly bioactive and display higher compactness and hardness with respect to the counterparts produced by conventional sintering methods.

Keywords: Composites, Hydroxyapatite, Bioactive glasses, spark plasma sintering, Mechanical properties.

1. Introduction

The repair of osseous defects caused by tumors, traumatic events or inflammatory diseases is a common clinical problem. Current lines of treatment such as autogenous bone grafts, which involve the transplantation of bone from another part of the patient, or allografts, where bone tissue is taken from donors or cadavers, are affected by specific drawbacks, i.e., donor site morbidity, disease transmission risks, high costs and potential complications like infections [1, 2]. In the last 40 years several research works have been devoted to develop specific synthetic alternatives for the replacement of damaged or lost bones. In this context, hydroxyapatite (HA), which belongs to the calcium phosphates group, plays a prominent role in oral, maxillofacial and orthopaedic surgery since the 1980s [3, 4]. Thanks to its similarity to the biological apatite, which constitutes the mineral phase of hard tissues, HA exhibits excellent biocompatibility and osteoconductivity, as it is able to promote, *in vivo*, bone tissue apposition to its surface. HA has been extensively used in form of cements, powders and granules to produce bone fillers and synthetic bone

grafts for biomedical applications. Unfortunately, the poor mechanical performance of HA (in particular the tensile strength and fracture toughness) makes its use difficult in bulk form when load bearing capacity is required. As a consequence, for such applications, HA utilization is mainly confined to the deposition of bioactive coatings on metallic implants [5 – 8].

The disadvantages associated to the use of HA also include the high sintering temperatures typically required for obtaining bulk products [9, 10]; moreover, the reactivity of this material at body temperature and physiological pH is typically low, consequently the osseointegration rate of HA-based grafts, which should match the rate of growth of the new tissue, is also rather modest [7, 11]. This fact can be particularly detrimental for the production of HA scaffolds for bone tissue engineering, which should resorb in a predictable way, at the same rate as the tissue is repaired.

In order to overcome these limitations, several investigations have been addressed to the preparation of HA-based composites with bioactive glasses as second phase. Most of these studies involved the use of 45S5 Bioglass® (45S5), the first bioactive glass developed by Larry Hench in 1969 [12]. 45S5 is a degradable glass in the Na_2O–CaO–SiO_2–P_2O_5 system, and it is able to form a chemical bond with soft tissues as well as with bone. In general, bioactive glasses bond to bone more rapidly than other bioceramics. Moreover, *in vitro* studies demonstrated that the dissolution products (e.g. Si, P, Ca) of 45S5 stimulate osteoblasts proliferation and seem to induce angiogenesis and neo-vascularization [13].

The production of HA/bioactive glass composites opens intriguing scenarios, since it allows to go beyond the intrinsic limits of the ceramic and glassy phases when considered singularly [4]. On the one hand, by varying the volume fractions of the two constituents, it is possible to control the bioactivity and the dissolution rate of the resulting material, so that innovative systems with tailored biological properties can be obtained. In addition, the use of glasses may be further exploited to incorporate specific ions, such as fluorine, silicon, magnesium or strontium, within the lattice of HA, with the aim to reproduce the composition of the biological apatite, which is intrinsically nonstoichiometric and calcium-deficient with many di- and tri-valent ion substitutions

[14]. Furthermore, the glass may act as sintering aid, thus promoting the densification of the composite powders [9, 10].

One of the main issues concerning the production of HA/bioactive glasses composites regards the thermal treatment which is necessary to sinter them. The densification of 45S5-based composites by pressureless sintering usually requires temperatures up to 1300 °C, which exceeds the crystallization temperature of the glassy phase. On the one hand, the crystallization of the glass has an adverse effect on the sintering process, thus limiting the densification of the final system which may be prone to unwanted residual porosity. Moreover, the HA decomposition and/or reactions between glass and apatite during the thermal treatment was also observed. Finally, the crystallization of the glassy phase may reduce its bioactivity [3, 9, 10, 15].

Several investigations have been devoted to understand how to tailor the glass formulation with the aim to prevent crystallization [16–18]. In recent years, a novel class of silicate glasses with lower tendency to crystallize with respect to 45S5 were produced and employed to develop HA-based composites. In particular the so-called BG_Ca/Mix system – a CaO-rich, K_2O modified glass composition – was specifically formulated as an alternative to 45S5 to be used whenever thermal treatments on bioactive glasses are required [19, 20]. A crystallization temperature of 880 °C is reported for BG_Ca/Mix, while 45S5 starts to crystallize at temperatures as low as 610 °C [21]. BG_Ca/Mix powders were recently used to produce various HA-based composites containing up to 70 wt.% of HA [22, 23]. Although it was possible to sinter the novel samples at a lower temperature with respect to HA/45S5 composites with the same HA/glass proportion, the composites with higher amounts of HA suffered for some residual porosity and poor mechanical properties. For these reasons, several efforts have been made to identify more efficient powder densification techniques, as an alternative to classical sintering.

In this regard, spark plasma sintering (SPS), also referred to as pulsed electric current sintering (PECS) or field-assisted sintering technique (FAST), represents a more effective consolidation method with respect to conventional pressureless and hot-pressing approaches [24]. Briefly, during SPS, an electric current flows through the graphite mould

containing the processing powders, that are therefore heated very fast by Joule effect. The simultaneous application of a mechanical load allows for the rapid obtainment of highly dense samples. Compared to alternative sintering methods, SPS has two main advantages: firstly, it makes processing time significantly shorter; secondly, it requires relatively lower temperatures to reach high consolidation levels. Consequently, SPS is beneficial in sintering processes where crystallization phenomena, grain growth, and/or phases decomposition have to be avoided or minimized.

Based on these considerations, two studies aimed to the consolidation by SPS of three different commercial HA powders [25] as well as 45S5 and BG_Ca/Mix bioactive glasses [26] were recently carried out. In particular, the full densification of HA CAPTAL® powders was achieved after 5 min dwell time at 1200°C and the resulting product does not present any secondary phase [25]. Moreover, concerning the bioglass powders, completely dense and fully amorphous BG_Ca/Mix materials were produced by SPS at 730°C in 2 min holding time [26].

In this work, the SPS technique is employed for the first time to produce HA-based composites with BG_Ca/Mix glass as second phase. Specifically, a systematic study is conducted to identify the optimal sintering conditions for preparing highly dense composites by considering three different HA/BG_Ca-Mix proportions. The obtained bulk products are then characterized from the compositional, microstructural and mechanical points of view. Finally, the bioactivity of the composites is investigated *in vitro* in a simulated body fluid solution.

2. Materials and Methods

2.1 Composites preparation

The raw powder reagents (commercial SiO_2, Na_2CO_3, $CaCO_3$, K_2CO_3, $Ca_3(PO_4)_2$ by Carlo Erba Reagenti, Rodano-Milano, Italy) were melted at 1450 °C for 1 hour to produce BG_Ca/Mix (composition: 47.3 mol% SiO_2, 45.6 mol% CaO, 2.3 mol% K_2O, 2.3 mol% Na_2O, and 2.6 mol% P_2O_5). Subsequently the melt was quenched in room-temperature water to obtain a frit which was dried at 110 °C for 12 hours and then milled into powder (grain

size < 45 μm). BG_Ca/Mix and commercial HA powders (CAPTAL® Hydroxylapatite, Plasma Biotal Ltd, UK) were accurately mixed in a plastic bottle using a rolls shaker for 6 hours in order to prepare the following set of composites:

- 80 wt.% BG Ca/Mix and 20 wt.% HA powders ("80BG_20HA");
- 50 wt.% BG Ca/Mix and 50 wt.% HA powders ("50BG_50HA");
- 30 wt.% BG Ca/Mix and 70 wt.% HA powders ("30BG_70HA").

Moreover, SPSed pure HA were prepared and subsequently used as a control in the investigation of the composites' bioactivity (see next paragraphs). The sintering conditions for the production of the HA samples have been previously reported and discussed in Ref. [25].

2.2 Spark plasma sintering of composite powders

Spark plasma sintering ~~Pulsed electric current sintering~~ experiments for the consolidation of 80BG_20HA, 50BG_50HA and 30BG_70HA ~~and 50BG_50HA~~ powders were performed by means of a SPS 515S equipment (Fuji Electronic Industrial Co., Ltd., Japan), which is based on the combination of an uniaxial press (50 kN maximum load) with a DC pulsed current generator (10 V, 1500 A, 300 Hz). The 12:2 ON/OFF pulses sequence was adopted, with the characteristic time of each pulse of about 3.3 ms. About 1.49, 1.53 or 1.56 g of 80BG_20HA, 50BG_50HA and 30BG_70HA-powders, respectively, were placed in a cylindrical die (outside diameter of 35 mm, inside diameter of 15 mm, and 30 mm high) equipped with two punches. All the tooling components consisted of AT101 graphite (Atal s.r.l., Italy). To facilitate sample release after SPS, a graphite foil with a 0.13 mm thickness (Alfa Aesar Karlsruhe, Germany) was placed between the pressed powder and the die/plungers walls. In addition, the die was covered with a graphite felt layer (3 mm thick, Atal s.r.l., Italy) to minimize thermal losses during the heating process.

Temperature measurement and control was performed using a K-type thermocouple (Omega Engineering Inc., USA) inserted in a small hole drilled at the die surface. The real-time evolution of a number of parameters, i.e., temperature, electric

current, voltage between the machine electrodes, applied load, and vertical sample displacement was recorded. It should be noted that the contribution of thermal expansion of the electrodes and graphite tooling has to be subtracted to the measured displacement to obtain sample shrinkage data (δ) [27], which will be considered hereafter.

During SPS runs, the temperature was first increased at a rate of 50°C/min until a value of 100°C lower than the holding temperature (T_D) was achieved. Afterwards, the T_D level was reached at a lower heating rate (10°C/min) to minimize overshooting problems. The effect of the dwell temperature was investigated in the range 730-1150°C. The sample was kept at the sintering temperature for a time interval (t_D) varying from 3 sec to 10 min. The applied mechanical pressure was varied from 16 to 30 MPa. It should be noted that the sintering conditions adopted in the present work were selected based on the results recently obtained when the SPS apparatus was used to consolidate separately ~~on~~ the two ~~separate~~ composite constituents. In particular, the less severe conditions needed to obtain full dense HA and BG_Ca/Mix samples were 1200°C, 5 min and 30 MPa [25] and 730°C, 2 min, and 16 MPa [26], respectively.

Finally, sintered disks with diameter of 14.7 mm and thickness of about 3 mm were obtained. For the sake of reproducibility, each experiment was repeated at least twice.

Densities of polished SPSed samples were determined by the Archimedes method. The theoretical densities of the 80BG_20HA, 50BG_50HA and 30BG_70HA systems, i.e., 2.915, 3.015 and 3.074 g/cm^3, respectively, were calculated using a rule of mixture [28]. In this regard, ~~a~~ density values of 3.16 g/cm^3 for HA and 2.86 g/cm^3 for BG_Ca/Mix were considered.

Phase composition of differently sintered composites was determined by XRD analysis using a Philips PW 1830 X-rays diffractometer (Philips PW 1830, Almelo, The Netherlands) equipped with a Ni filtered Cu K_α radiation (λ=1.5405 Å).

2.3. Microstructural and Mechanical characterization of the composites

Among the produced composites, a subset has been selected, based on high values of density, for further characterizations. The bulk products examined are listed in Table 1 along with the corresponding SPS conditions and relative densities.

The mirror polished cross-sections of the obtained samples were observed in an Environmental Scanning Electron Microscope (ESEM Quanta 2000, FEI Co., Eindhoven, The Netherland) operated in low-vacuum conditions (~0.5 Torr). Qualitative compositional analyses were performed by means of X-ray energy dispersion spectroscopy (X-EDS) (Inca, Oxford Instruments, UK).

Vickers micro-indentation tests (Wolpert Group, Micro-Vickers Hardness Tester digital auto turret, Mod. 402MVD) were performed on the polished cross-sections in order to determine the Vickers hardness of the samples. For each material, at least 15 clear and crack-free indentations were performed by applying a maximum load of 100 g_f for 15 s [29].

2.4. Investigation of the in vitro bioactivity

The *in vitro* bioactivity of the produced samples was evaluated by soaking them in an acellular simulated body fluid solution for different time periods, according to the procedure developed by Kokubo et al [30]. For each set of produced composites one sample was tested. The samples were soaked in flasks containing 25 ml of SBF and stored at 37 °C in an incubator. The solution was refreshed every about 48 hours. The contact between composites and the solution was interrupted after 3, 7 and 14 days. The specimens were then rinsed with water and left to dry for 24 hours at room temperature. The samples' surface was observed by SEM in order to investigate microstructural changes that occurred after immersion and the possible precipitation of hydroxyapatite. Moreover, micro-Raman spectroscopy was performed, using a a Jobin–Yvon Raman Microscope spectrometer (Horiba Jobin–Yvon, Villeneuve D'ascq, France) equipped with a 632.8 nm-wavelength He–Ne diode laser.

3. Results and Discussion

3.1. Powders sintering

The densification behaviour of the three composites produced under the same SPS conditions (T_D=800°C, t_D=10 min, P=30 MPa) is reported in **Figure 1**. The corresponding temperature profile is also shown. Similar gradual and modest changes of the δ parameter are observed for the three composite powders when they are exposed to thermal levels below 700°C. On the other hand, as the temperature was further augmented, the sample shrinkage progressively increases at a higher rate, especially for the composite powders richer in BG_Ca/Mix. At the end of the experiments, the relative densities (average values) of the obtained sintered 80BG_20HA, 50BG_50HA and 30BG_70HA products were 98.075, 88.4 and 73.8, respectively. These outcomes are perfectly consistent with the composition of the starting powders, i.e. sample density increases as the fraction of the constituent glass is progressively augmented.

A systematic investigation was conducted to identify, for the three composites under consideration, the less severe SPS conditions able to guarantee the preparation of nearly full dense products. The results obtained for the 80BG_20HA system are shown in **Figure 2(a)**. As expected, it is possible to notice that an increase of the holding temperature, dwell time and/or applied pressure parameters promotes powders consolidation, so that the conditions for producing samples having density higher than 96% are identified. Specifically, such densification degree can be reached for T_D values above 770°C when t_D=10 min. As shown in **Figure 2(b)**, the XRD pattern of the resulting product shows a broad hump, that evidences the still amorphous nature of BG_Ca/Mix, although the small peak of α-$CaSiO_3$ provides an indication of the incipient crystallization of the bioglass. The latter phenomenon is significantly enhanced as the sintering temperature was increased to 800°C. Indeed, peaks intensity related to α-$CaSiO_3$ increases markedly. In addition, a smaller amount of β-$CaSiO_3$ was also found and, more important, the amorphous hump basically disappeared from the XRD pattern.

Crystallization phenomena can be mitigated if the holding time is sufficiently shortened while maintaining the thermal levels unchanged. In fact, as reported in **Figure**

2(c), no additional crystalline phases, other than HA, are detected by XRD in the 95.7% dense product obtained by SPS after 3 sec at 780°C. However, a small amount of α-$CaSiO_3$ was formed when the temperature was raised to 800°C to improve powders densification up to 96.7%, considering the same t_D and P conditions. Nonetheless, the XRD analysis revealed that in the latter case the sintered product still exhibits an amorphous character. In order to further increase the end product densities, higher temperatures or applied pressures were also considered. However, samples breakage correspondingly occurred during the SPS process.

Based on the results described above, it is possible to state that T_D=800°C, t_D= 3 sec, and P=30 MPa are the more convenient SPS conditions, among those ones investigated in the present work, to produce 80BG_20HA samples with average densities higher than 96.5%, where the crystallization of the bioglass is just at the early stage.

Accordingly, the optimal holding temperature for the other two composite systems examined in this work was identified by setting the t_D and P values equal to 3 sec and 30 MPa, respectively.

Specifically, the data obtained for the 50BG_50HA sample are plotted in **Figure 3**. As expected, due to the presence of a larger amount of HA, the consolidation of these powders required higher thermal levels with respect to the previous system. In particular, as reported in **Figure 3(a)**, a 90.5% dense 50BG_50HA sample (average value) was produced by SPS when the holding temperature was set at 850°C. Under such conditions, no additional phases were evidenced by the XRD analysis. On the other hand, both α- and β-$CaSiO_3$ were found in the slightly denser compacts obtained at 950°C (relative density of about 92.5%). In addition, it can be observed that a further temperature increase to 1000°C determined a partial transformation of α- to β- $CaSiO_3$. A product approximately 98% dense was correspondingly obtained.

Powder consolidation gets more difficult when the fraction of HA in the composite mixture is further increased, so that the occurrence of crystallization phenomena is favored by the higher T_D values required to reach the desired densification levels. In particular, as reported in **Figure 4(a)**, still very porous 30BG_70HA products resulted

when the holding temperature was set at 950°C. Moreover, as evidenced by the corresponding XRD pattern shown in **Figure 4(b)**, such condition was anyway sufficient to determine a significant crystallization from the glassy phase with the formation of $CaSiO_3$, in both the α- and β- forms. The progressive increase of the temperature strongly promoted powder consolidation, so that fully dense products are obtained at 1150°C.

Based on the observed outcomes, the lowest holding temperatures, among those investigated, sufficient to reach a density of 96.5% or higher for 80BG_20HA, 50BG_50HA and 30BG_70HA specimens by SPS (tD= 3 sec, P= 30 MPa) are 800, 1000 and 1150°C, respectively.

These findings are well in agreement with the results recently obtained when HA and BG_Ca/Mix powders were separately processed by SPS [25, 26]. First of all, the beneficial role played by the glass component as sintering aid is evidenced. Indeed, it was found that the SPS conditions needed for the nearly full consolidation of BG free HA were T_D= 1200°C, t_D= 5 min and P=30 MPa [25]. On the other hand, the same goal could be reached after only 3 sec at 1150°C or lower temperatures, when at least 30% of BG_Ca/Mix are added to the mixture. Moreover, based on XRD analysis, HA did not decompose when the three composites systems under investigation were processed by SPS. This is an important outcome, since the formation of β-TCP or other secondary phases from the HA decomposition**,** which tends to occur in the powders undergoing SPS when operating at relatively higher temperatures, might reduce the bioactivity of the resulting sample. Indeed, recent studies evidenced that β-TCP exhibits a rather lower aptitude, with respect to HA, to promote the formation of new phosphate phases in the bioceramic surface during both *in vitro* (simulated body fluid) and *in vivo* experiments [31].

As for the behavior of the BG_Ca/Mix constituent, it is observed that the massive composite samples with relative densities equal or higher than 96% are generally obtained in presence of a certain bioglass crystallization. The only exception is represented by the 80BG_20HA system processed for 3 sec at 780°C. On the other hand, a slight temperature increase to 800°C produced, other than an improvement of powder densification, also the formation of a small amount of α-$CaSiO_3$. This feature was relatively more accentuated

when the other two composites – richer in HA – were taken into account. The latter result is readily associated to the fact that, when the relative amount of HA in the composite is progressively augmented, the dwell temperatures set to consolidate powder mixtures have to be higher. In particular, the optimal T_D values identified in this work to achieve density levels above 96% for the 80BG_20HA, 50BG_50HA and 30BG_70HA systems are 800, 1000 and 1150°C, respectively. Therefore, the crystallization of the bioglass is correspondingly favoured, as clearly confirmed by the XRD analyses of the resulting sintered samples. In particular, the temperature levels up to 1150°C needed to obtain nearly full dense 30BG_70HA materials have further promoted the formation of $CaSiO_3$, also in the β- configuration, from the glassy phase.

Nonetheless, it should be noted that devitrification phenomena as well as HA decomposition would occur at a significant higher degree if classic sintering methods, less efficient than SPS, and/or other bioglass compositions, displaying higher tendency to crystallize with respect to BG_Ca/Mix, are used.

3.2. Microstructural and Mechanical characterization

The bulk products examined by SEM are listed in Table 1 along with the corresponding SPS conditions and relative densities. **Figure 5** and **Figure 6** display some representative micrographs of the cross sections of the produced composites. Although the samples are adequately densified, some residual pores are still present. Nevertheless, several features visible in the sample images can be attributed to the preferential removal of HA-rich particles during the polishing step. This aspect is more evident when observing the micrograph of the 80BG_20HA#1 cross section reported in **Figure 7(a)** and the corresponding X-EDS maps, which show the distribution of P, representative of HA in the composite, and Si, associate to the glass. In fact, the damaged areas in **Figure 7(a)** can be mainly identified as HA, since they are particularly poor in Si and rich in P. Beside this feature, the cross section images show areas with different brightness (see, in particular, **Figure 8**): light areas should be ascribed to HA, while dark ones are representative of

BG_Ca/Mix. It should be noted that the 30BG_70HA#2 sample looks particularly compact, with no traces of porosities. This finding is quite interesting, since the counterparts produced by traditional sintering suffered from widespread residual porosity and poor mechanical performance [22, 23]. On the contrary, the SPS technique allowed to obtain fully dense and compact samples, regardless of the HA/glass proportions. This fact is further confirmed by the micro-hardness values of the produced samples, which are reported in **Table 1**. It should be stressed that a direct comparison between the mechanical performance of the produced composites is not straightforward, since the samples differ in composition, density, microstructure, degree of crystallization of the glassy phase and mechanical properties of the formed crystalline phases. Nonetheless, on the basis of previous results obtained in the literature on the same HA and bioglass systems processed either separately by SPS or in combination using a diverse sintering technique, some considerations can be made in this context. First of all, it is important to underline that the SPSed composites obtained in the present work show significantly higher hardness with respect to samples with the same HA/glass ratio prepared by traditional sintering. For sake of comparison, a Vickers hardness of 368.1 ± 83.3 is reported in Ref. [23] for 80BG_20HA composites produced by means of traditional sintering. Furthermore, the residual porosity present in 30BG_70HA samples obtained using the latter approach did not permit the obtainment of reliable data for their micro-hardness [23]. In fact, indentation techniques are very sensitive to local defects, such as pores. It should be finally noted that 50BG_50HA counterparts have not been produced yet by conventional sintering.

The results reported in Table 1 indicate that the 30BG_70HA_#2 samples, which are characterized by a particularly high compactness ($\rho > 99.9\%$) and a defects-free microstructure (see **Figures 6(f)** and **8(a)**), show the best performance also in terms of Vickers hardness. In contrast, the 30BG_70HA_#1 specimen has the lowest hardness among the samples examined in the present work. This result can be likely due to its lower density ($\rho = 96.9\%$) and the relatively higher HA content. In this regard, it should be noted that two recent investigations focused on HA and BG_Ca/Mix processed separately by

SPS, revealed that the micro-hardness data for BG_Ca/Mix were slightly higher than those ones found for HA (see Ref. [25, 26] for details). Such finding is consistent to the lower hardness displayed by 30BG_70HA_#1 samples with respect to those ones obtained for 80BG_20HA_#1 and 80BG_20HA_#3 specimens, which have the same density but are characterized by a higher BG_Ca/Mix content. The hardness of 50BG_50HA samples is rather similar to the 80BG_20HA ones, since the negative effect due to the lower BG_Ca/Mix fraction in the 50BG_50HA composite is probably counterbalanced by its relatively higher density (ρ = 98.6%). For what concerns the 80BG_20HA samples, the 80BG_20HA_#3 has the best performance. However, in this case the analysis is complicated by the fact that the different degree of crystallization of BG_Ca/Mix in the composites should be taken in account. For example, the results reported in Figure 2 show that the amorphous nature of BG_Ca/Mix is better retained in 80BG_20HA#3 than in 80BG_20HA#2, although the latter one is denser. This fact could explain the slightly higher hardness of 80BG_20HA#3 with respect to that of 80BG_20HA#2.

3.3 In vitro bioactivity of the composites

Since the SPS method has been used for the first time to produce the composite systems under consideration, some preliminary results relative to the evaluation of their bioactivity are also reported. In this regard, the reactivity of the samples was investigated *in vitro* according to the procedure by Kokubo et al [30]. This method, which aims to evaluate the apatite formation ability of bioactive glasses and bioceramics in SBF, is widely used as a preliminary screening test of the samples' bioactivity.

After soaking in SBF, the characterization of the produced composites revealed the formation of apatite precipitates, which progressively spread on the samples' surface. In **Figures 9** and **10** it is possible to observe that the 80BG_20HA#1 surface, after 7 and 14 days of immersion, respectively, is covered by aggregates of spherical particles with the typical apatite morphology. The X-EDS analysis (**Figure 9(b, c)**) performed on the precipitates revealed that such aggregates are particularly rich in calcium and

phosphorous. Some Si is also detectable, due to the glassy phase underneath the precipitates and to the possible formation of a silica gel layer, according to the models which describe the reaction mechanisms of bioceramics and bioactive glasses in SBF reported by the literature [12, 32, 33]. The nature of the globular precipitates was further investigated by micro-Raman spectroscopy. The Raman spectrum acquired on the 80BG_20HA#1 composite after 14 days in SBF, which is shown in **Figure 11**, looks rather similar to that of commercial apatite [34]. It is possible to observe three peaks, i.e. an intense and sharp peak at ~960 cm^{-1} and two peaks with lower intensity at ~430 cm^{-1} and ~590 cm^{-1}, which are ascribable to the PO_4 vibrations [35]; a further peak at ~1070 cm^{-1} can be referred to the stretching of carbonate groups [36]. In conclusion, it is possible to identify the precipitates on 80BG_20HA#1 as carbonated hydroxyapatite: this confirms the *in vitro* bioactivity of the prepared samples. Previous investigations have demonstrated that dense HA produced by SPS showed strong ability to induce hydroxyapatite formation *in vitro* [37, 38]. Nevertheless, it should be stressed that the development of such apatite layer on the composites under consideration could be mainly ascribable to BG_Ca/Mix, which revealed significantly higher *in vitro* reactivity. This fact is clearly evidenced in Figure 12, which shows the surfaces of SPSed bioglass-free HA, 30BG_70HA, 50BG_50HA and 80BG_20HA after soaking in SBF for three days. It is possible to observe that the relative content of apatite precipitates on the samples' surface increased with the increasing amount of BG_Ca/Mix in the sample. In particular, the newly formed apatite completely covered the 80BG_20HA surface, i.e., the sample with the highest content of glass. Therefore, the addition of BG_Ca/Mix may be used to modify the dissolution of the final system and to tune its biological response to the specific clinical application. It should be stressed that the latter aspect probably represents the most important advantage associated to the use of silicate-glass/HA composites. Moreover, thanks to its low tendency to crystallize, the BG_Ca/Mix in the composites maintained almost completely its amorphous nature, with positive effects in terms of the resulting bioactivity; on the other hand, the partial crystallization of BG_Ca/Mix to α- and β-$CaSiO_3$, which belong to the family of wollastonite ceramics, is not detrimental regarding the HA-forming ability in

SBF, since such crystalline phases also display a bioactive character, as reported in the literature [39–42]. For example, Liu *et al.*, who investigated the bioactivity of wollastonite coatings deposited on titanium, observed the formation of hydroxycarbonate apatite on the coatings' surface after 1 day in SBF [39]. A good bioactivity was also shown by dense β-$CaSiO_3$ ceramics produced through SPS and subsequently tested in SBF for increasing soaking times [40]. The bioactivity in SBF of both α- and β-$CaSiO_3$ has been confirmed by Siriphannon *et al* [41] who also discussed about the differences *in vitro* between the two phases. Finally, other studies demonstrated that α- and β-$CaSiO_3$ ceramics are also able to support cell attachment, proliferation and differentiation [42].

It is important to note that the findings concerning bioactivity of the obtained composites are qualitatively analogous to those ones reported for their counterparts produced by means of traditional sintering [22, 23]. However, the composites processed by SPS , in particular the 30BG_70HA and 50BG_50HA samples, exhibit far higher compactness, hardness and density. For these reasons, the SPS technology looks very promising for the production of HA/bioactive glass composites.

4. Conclusions

In this work SPS was employed to produce almost completely dense and highly bioactive composites based on different mixtures of HA and of BG_Ca/Mix, a recently developed CaO-rich silicate bioactive glass. The produced samples are very compact and significantly denser ($\rho \geq 96\%$) with respect to the counterparts produced by conventional sintering methods. In particular, for the first time, a set of HA/BG_Ca-Mix samples (70wt.% HA) with a density near to the theoretical value has been successfully obtained. Furthermore, thanks to the low tendency to crystallize of the innovative BG_Ca/Mix, it was possible to reduce the devitrification of the glassy phase in the samples, with beneficial effects in terms of the resulting *in vitro* bioactivity. Although a certain degree of glass crystallization is typically observed in fully dense composite samples, crystallization phenomena, as well as HA/glass reactions and HA decomposition, are considerably lower

with respect to those observed when classic sintering methods and/or other bioactive glass compositions are used. In conclusion, (1) SPS provides an efficient tool to produce HA-based composites with bioactive glass as second phase, and (2) BG_Ca/Mix is confirmed to be particularly useful whenever a thermal treatment is required to produce the final system. Further studies regarding the biocompatibility of the obtained samples as well as the production by SPS of HA/BG_Ca-Mix composites modified with ions of biological interest, such as strontium and/or magnesium, are under investigation. The results will be the subject of future works.

5. Acknowledgments

The financial support for this work from Regione Autonoma della Sardegna (Italy), L.R. n.7/2007, CUP n. F71J11001070002, is gratefully acknowledged. One of us (Luca Desogus) has performed his activity in the framework of the International PhD in Innovation Sciences and Technologies at the University of Cagliari, Italy.

6. References

1. R.F. LaPrade, J.C. Botker. Donor-site morbidity after osteochondral autograft transfer procedures. Arthroscopy 20 (2004) e69–e73.
2. S.H. Palmer, C.L. Gibbons, N.A. Athanasou. The pathology of bone allograft. J Bone Jt. Surg. Br. 81 (1999) 333–335.
3. D. Bellucci, A. Sola, V. Cannillo. Hydroxyapatite and tricalcium phosphate composites with bioactive glass as second phase: State of the art and current applications. J. Biomed. Mater. Res. Part A 104A (2016) 1030–1056.
4. S. Samavedi, A.R. Whittington, A.S. Goldstein. Calcium phosphate ceramics in bone tissue engineering: A review of properties and their influence on cell behavior. Acta Biomater. 9 (2013) 8037–8045.

5. G. Bolelli, D. Bellucci, V. Cannillo, L. Lusvarghi, A. Sola, N. Stiegler, P. Müller, A. Killinger, R. Gadow, L. Altomare, L. De Nardo. Suspension thermal spraying of hydroxyapatite: Microstructure and in vitro behaviour. Mater. Sci. Eng. C 34 (2014) 287–303.
6. P. Habibovic, T.M. Sees, M.A. van den Doel, C.A. van Blitterswijk, K. de Groot. Osteoinduction by biomaterials—Physicochemical and structural influences. J. Biomed. Mater. Res. 77 (2006) 747–762.
7. M. Bohner. Calcium orthophosphates in medicine: From ceramics to calcium phosphate cements. Injury 31 (2000) D37–D47.
8. K.J.L. Burg, S. Porter, J.F. Kellam. Biomaterial developments for bone tissue engineering. Biomaterials 21 (2000) 2347–2359.
9. J.D. Santos, R.L. Reis, F.J. Monteiro, J.C. Knowles, G.W. Hastings. Liquid phase sintering of hydroxyapatite by phosphate and silicate glass additions: Structure and properties of the composites. J. Mater. Sci. Mater. Med. 6 (1995) 348–352.
10. J.D. Santos, P.L. Silva, J.C. Knowles, S. Talal, F.J. Monteiro. Reinforcement of hydroxyapatite by adding P_2O_5-CaO glasses with Na_2O, K_2O and MgO. J. Mater. Sci. Mater. Med. 7 (1996) 187–189.
11. P. Proussaefs, H.S. Olivier, J. Lozada. Histologic evaluation of a 12-year-old threaded hydroxyapatite-coated implant placed in conjunction with subantral augmentation procedure: a clinical report. J. Prosthet. Dent. 92 (2004) 17-22.
12. L.L. Hench. Bioceramics: From concept to clinic. J. Am. Ceram. Soc. 74 (1991) 1487–1510.
13. A.A. Gorustovich, J.A. Roether, A.R. Boccaccini. Effect of bioactive glasses on angiogenesis: a review of in vitro and in vivo evidences. Tissue Eng. Part B Rev. 16 (2010) 199-207.
14. J. Kolmas, A. Jaklewicz, A. Zima, M. Bućko, Z. Paszkiewicz, J. Lis, A. Ślósarczyk, W. Kolodziejski. Incorporation of carbonate and magnesium ions into synthetic hydroxyapatite: the effect on physicochemical properties. J. Mol. Struct. 987 (2011) 40–50.

15. J.C. Knowles, W. Bonfield. Development of a glass reinforced hydroxyapatite with enhanced mechanical properties. The effect of glass composition on mechanical properties and its relationship to phase changes. J. Biomed. Mater. Res. 27 (1993) 1591–1598.
16. J.J. Jones. Reprint of: Review of bioactive glasses: From Hench to hybrids. Acta Biomater. 23 (2015) S53-S82.
17. D. Bellucci, V. Cannillo, A. Sola. A new potassium-based bioactive glass: Sintering behaviour and possible applications for bioceramic scaffolds. Ceram. Int. 37 (2011) 145-157.
18. D. Bellucci, V. Cannillo, G. Ciardelli, P. Gentile, A. Sola. Potassium based bioactive glass for bone tissue engineering. Ceram. Int. 36 (2010) 2449-2453.
19. D. Bellucci, A. Sola, V. Cannillo. Low temperature sintering of innovative bioactive glasses. J. Am. Ceram. Soc. 95 (2012) 1313–1319.
20. D. Bellucci, V. Cannillo, A. Sola. Calcium and potassium addition to facilitate the sintering of bioactive glasses. Mater. Lett. 65 (2011) 1825–1827.
21. L. Lefebvre, J. Chevalier, L. Gremillard, R. Zenati, G. Thollet, D. Bernache-Assolant, A. Govin. Structural transformations of bioactive glass 45S5 with thermal treatments. Acta Mater. 55 (2007) 3305–3313.
22. D. Bellucci, A. Sola, V. Cannillo. Bioactive glass-based composites for the production of dense sintered bodies and porous scaffolds. Mater. Sci. Eng. C 33 (2013) 2138–2151.
23. D. Bellucci, A. Sola, A. Anesi, R. Salvatori, L. Chiarini, V. Cannillo. Bioactive glass/hydroxyapatite composites: Mechanical properties and biological evaluation. Mater. Sci. Eng. C 51 (2015) 196-205.
24. R. Orrù, R. Licheri, A.M. Locci, A. Cincotti, G. Cao. Consolidation/synthesis of materials by electric current activated/assisted sintering. Mat. Sci. Eng. R 63 (2009) 127-287.
25. A. Cuccu, S. Montinaro, R. Orrù, G. Cao, D. Bellucci, A. Sola, V. Cannillo. Consolidation of different Hydroxyapatite powders by SPS: optimization of the

sintering conditions and characterization of the obtained bulk products. Ceram. Intern. 41 (2015) 725-736.

26. L. Desogus, A. Cuccu, S. Montinaro, R. Orrù, G. Cao, D. Bellucci, A. Sola, V. Cannillo. Classical Bioglass® and innovative CaO-rich bioglass powders processed by Spark Plasma Sintering: a comparative study. J. Eur. Ceram. Soc. 35 (2015) 4277-4285.
27. A.M. Locci, R. Orrù, G. Cao, Z.A. Munir. Effect of ball milling on simultaneous spark plasma synthesis and densification of TiC-TiB_2 composites. Mat. Sci. Eng.A 434 (2006) 23-29.
28. F.L. Matthews, R. Rawlings. Composite Materials: Engineering and Science. Chapman & Hall, Great Britain; 1994.
29. G.D. Quinn, P.J. Patel, I. Lloyd, Effect of loading rate upon conventional ceramic microindentation hardness. J. Res. Natl. Inst. Stand. 107 (2002) 299-306.
30. T. Kokubo, H. Takadama. How useful is SBF in predicting in vivo bone bioactivity? Biomaterials 27 (2006) 2907–2915.
31. R. Xin, Y. Leng, J. Chen, Q. Zhang. A comparative study of calcium phosphate formation on bioceramics in vitro and in vivo Biomaterials 26 (2005) 6477-6486.
32. Q.Z. Chen, I.D. Thompson, A.R. Boccaccini. 45S5 Bioglass-derived glass-ceramic scaffolds for bone tissue engineering. Biomaterials 27 (2006) 2414–2425.
33. A.R. Boccaccini, Q. Chen, L. Lefebvre, L. Gremillard, J. Chevalier. Sintering, crystallisation and biodegradation behaviour of Bioglass-derived glass-ceramics. Faraday Discuss. 136 (2007) 27–44.
34. D. Bellucci, G. Bolelli, V. Cannillo, A. Cattini, A. Sola. In situ Raman spectroscopy investigation of bioactive glass reactivity: Simulated body fluid solution vs TRIS-buffered solution. Mater. Charact. 62 (2011) 1021–1028.
35. S. Koutsopoulos. Synthesis and characterization of hydroxyapatite crystals: A review study on the analytical methods. J. Biomed. Mat. Res. 62 (2002) 600–612.
36. A. Awonusi, M.D. Morris, M.M.J. Tecklenburg. Carbonate assignment and calibration in the Raman spectrum of apatite. Calcif. Tissue Int. 81 (2007) 46–52.

37. Y.W. Gu, K.A. Khor, P. Cheang. Bone-like apatite layer formation on hydroxyapatite prepared by spark plasma sintering (SPS). Biomaterials 25 (2004) 4127–4134.
38. A. Nakahira, M. Tamai, H. Aritani, S. Nakamura, K. Yamashita. Biocompatibility of dense hydroxyapatite prepared using an SPS process. J. Biomed. Mater. Res. 62 (2002) 550–557.
39. X. Liu, C. Ding, Z.Wang, Apatite formed on the surface of plasma-sprayed wollastonite coating immersed in simulated body fluid. Biomaterials 22 (2001) 2007–2012.
40. L.H. Long, L.D. Chen, S.Q. Bai, J. Chang, K.L. Lin. Preparation of dense β-$CaSiO_3$ ceramic with high mechanical strength and HAp formation ability in simulated body fluid. J. Eur. Ceram. Soc. 26 (2006) 1701–1706.
41. P. Siriphannon, Y. Kameshima, A. Yasumori, K. Okada, S. Hayashi, Formation of hydroxyapatite on CaSiO3 powders in simulated body fluid. J. Eur. Ceram. Soc. 22 (2002) 511–520.
42. S. Ni, J. Chang, L. Chou, W. Zhai. Comparison of osteoblast-like cell responses to calcium silicate and tricalcium phosphate ceramics in vitro. J. Biomed. Mater. Res. B Appl. Biomater. 80 (2007) 174–83.

Table 1. Samples, processing parameters, final density and Vickers hardness of the produced composites. Vickers hardness is expressed as mean value ± standard deviation. For sake of comparison, in Ref [23] a hardness of 368.1 ± 83.3 Vickers is reported for 80BG_20HA composites produced by means of traditional sintering.

Sample	**T_D, t_D**	**ρ [%]**	**HV [Vickers]**
80BG_20HA_#1	770°C, 10 min	96.9	539.5 ± 31.1
80BG_20HA_#2	800°C, 10 min	98.45	553.1 ± 25.4
80BG_20HA_#3	800°C, 3 sec	96.9	586.4 ± 20.8
50BG_50HA	1000°C, 3 sec	98.6	536.3 ± 29.7
30BG_70HA_#1	1100°C, 3 sec	96.9	456.4 ± 38.2
30BG_70HA_#2	1150°C, 3 sec	>99.9	634.7 ± 19.9

Figure 1. Example of the temperature-time profile and the corresponding sample shrinkage curves obtained during the consolidation of the three composite systems by SPS (T_D=800°C, t_D=10 min, P=30 MPa).

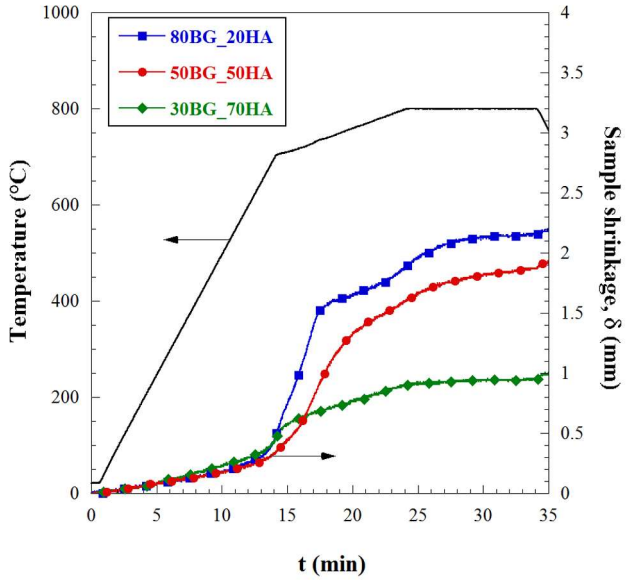

Figure 2. Effect of the sintering conditions on the relative density (a) of 80BG_20HA samples produced by SPS and the corresponding XRD patterns obtained at *P*=30 MPa when t_D=10 min (b) and t_D= 3 sec (c).

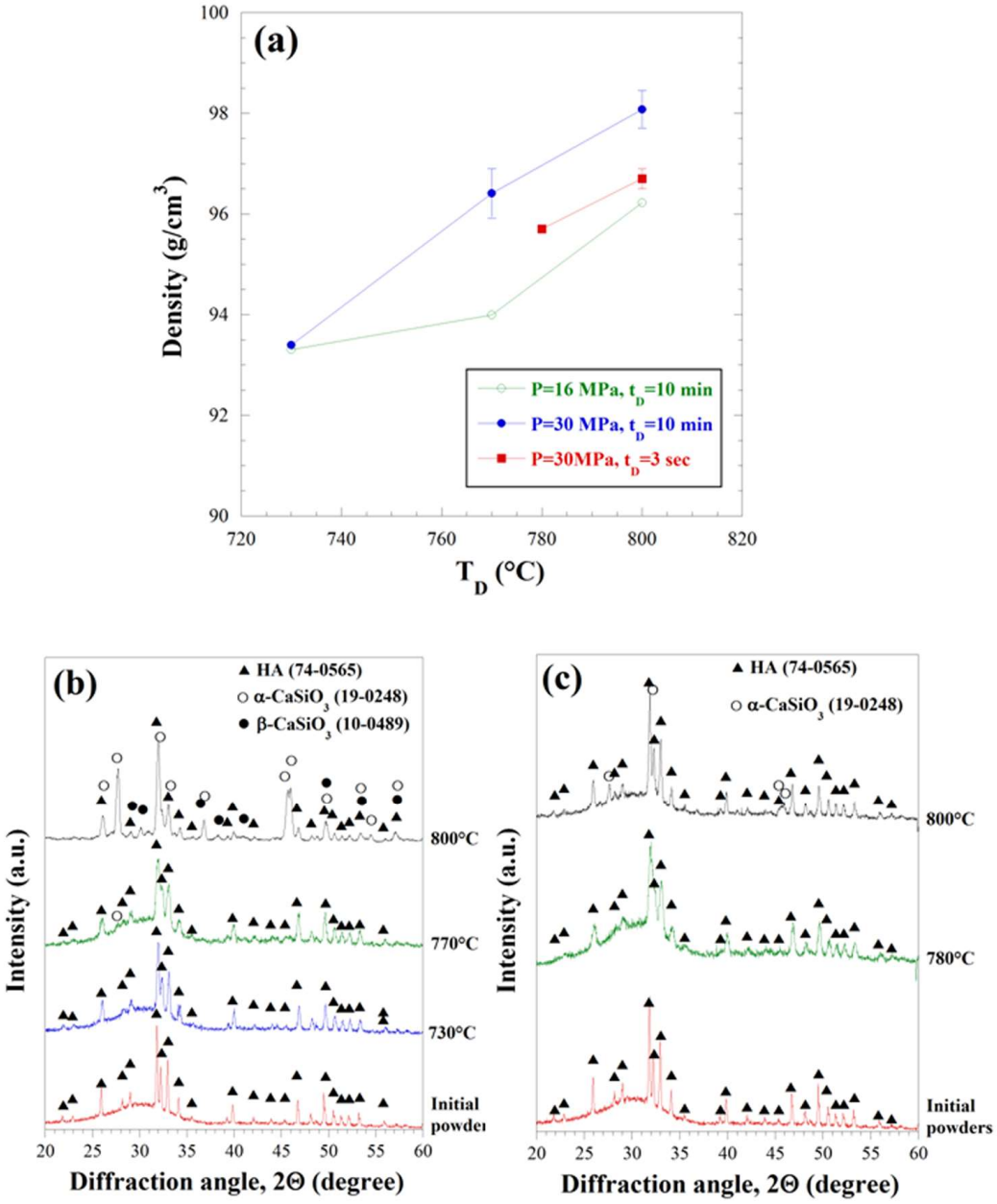

Figure 3. Effect of the sintering temperature (t_D= 3 sec, P=30 MPa) on the relative density (a) of 50BG_50HA samples produced by SPS and the corresponding XRD patterns (b).

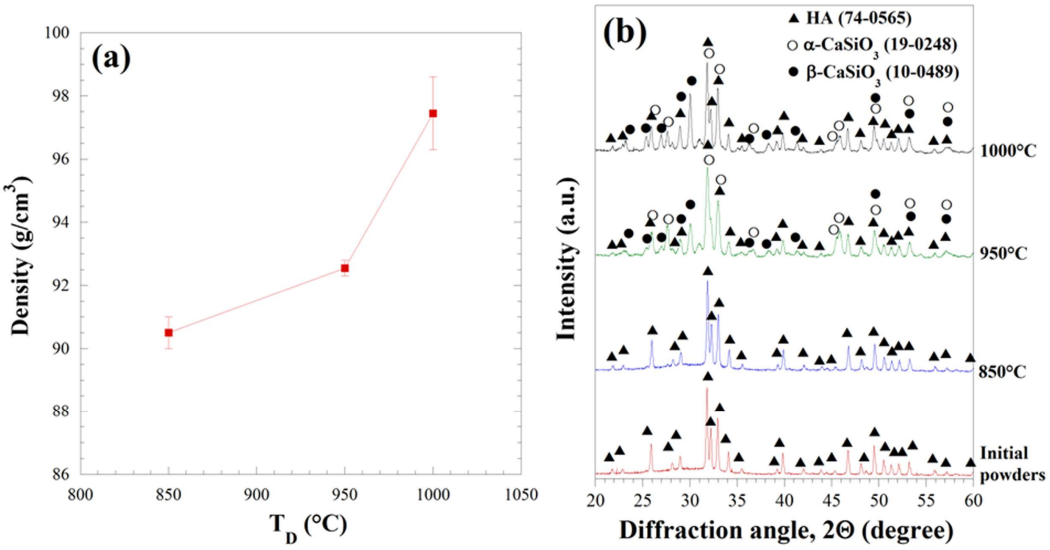

Figure 4. Effect of the sintering temperature (t_D= 3 sec, P=30 MPa) on the relative density (a) of 30BG_70HA samples produced by SPS and the corresponding XRD patterns (b).

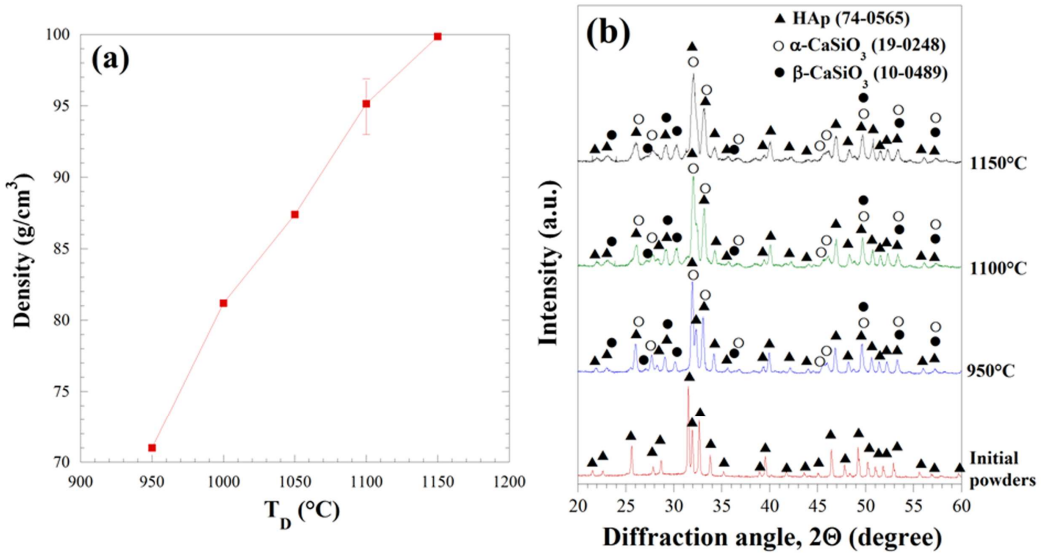

Figure 5. Cross sections of the produced composites.

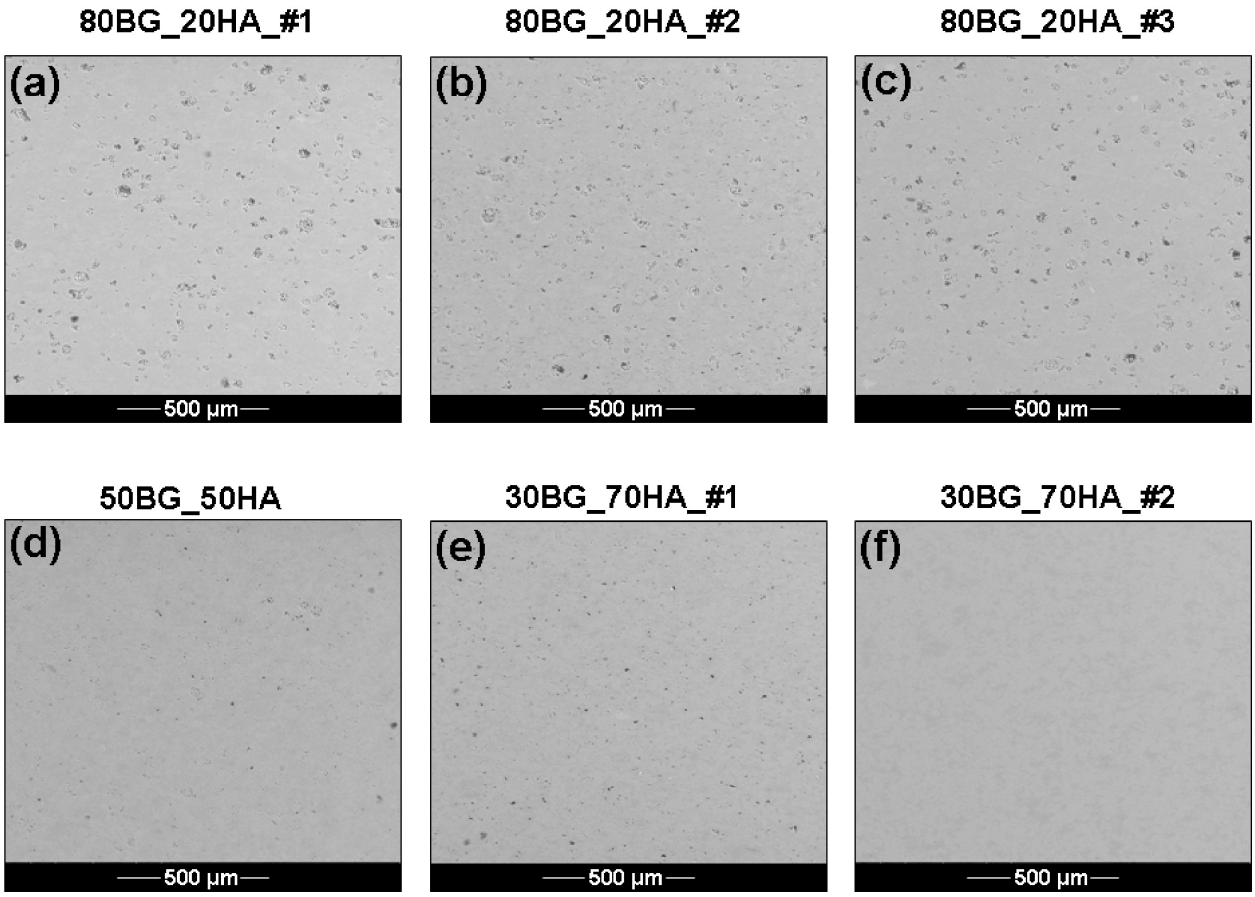

Figure 6. Cross sections of the produced composites: high magnification micrographs.

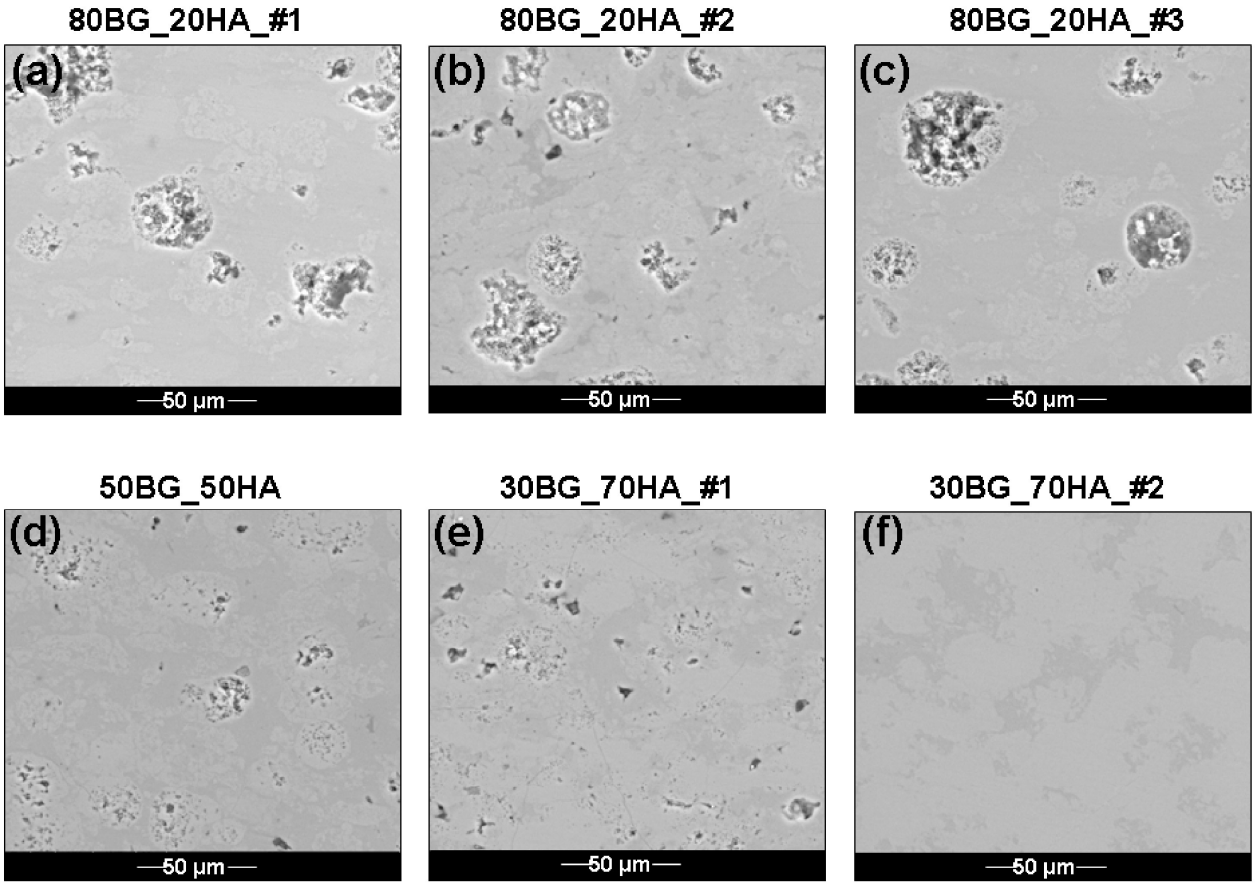

Figure 7. Micrograph of the 80BG_20HA#1 cross section (a) and corresponding X-EDS maps showing the distribution of Si (b) – representative of the glass – and P (c), representative of HA.

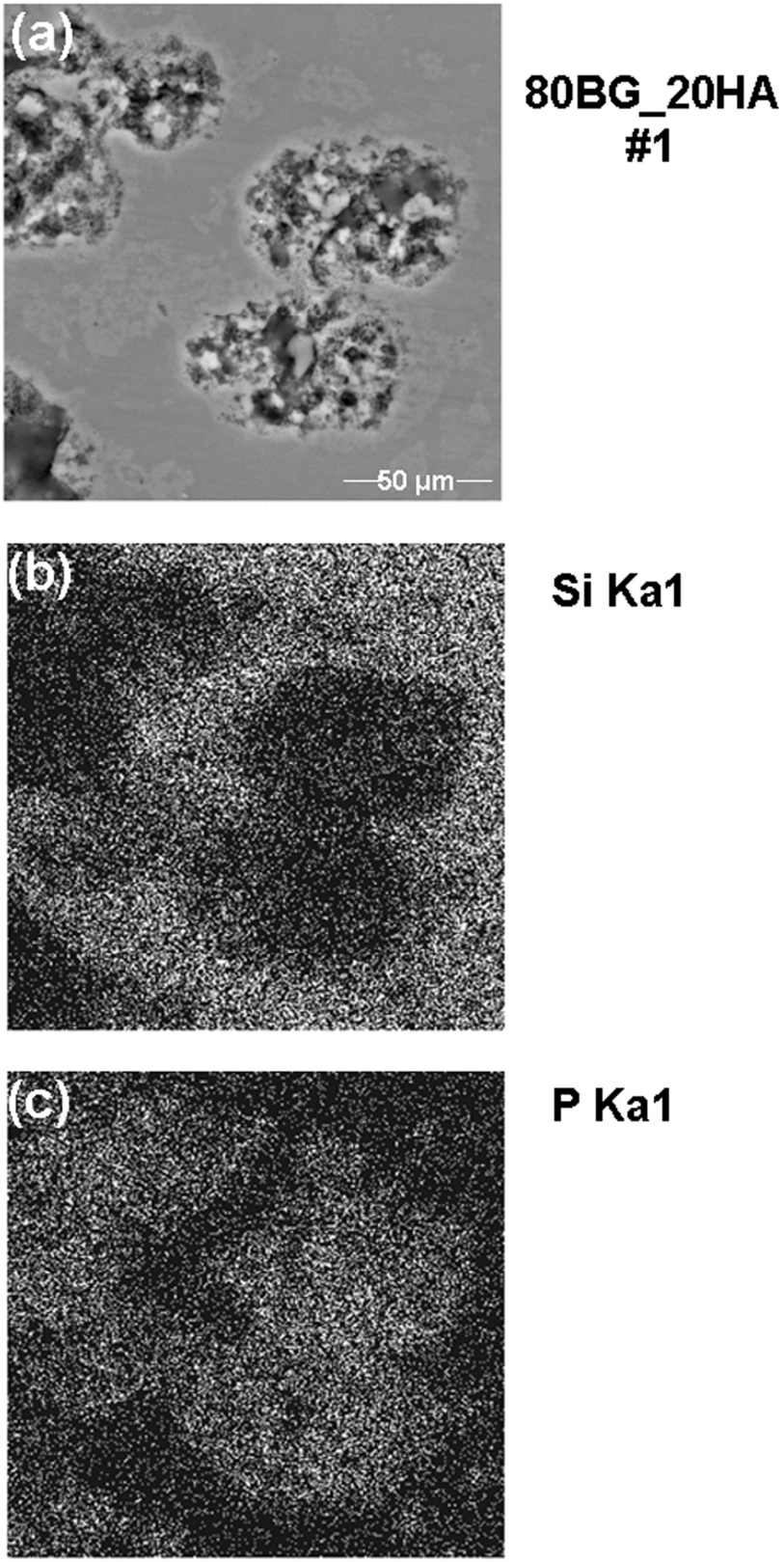

Figure 8. Micrograph of the 30BG_70HA#2 cross section (a) and results of the X-EDS analysis (b, c) performed on the areas indicated in (a).

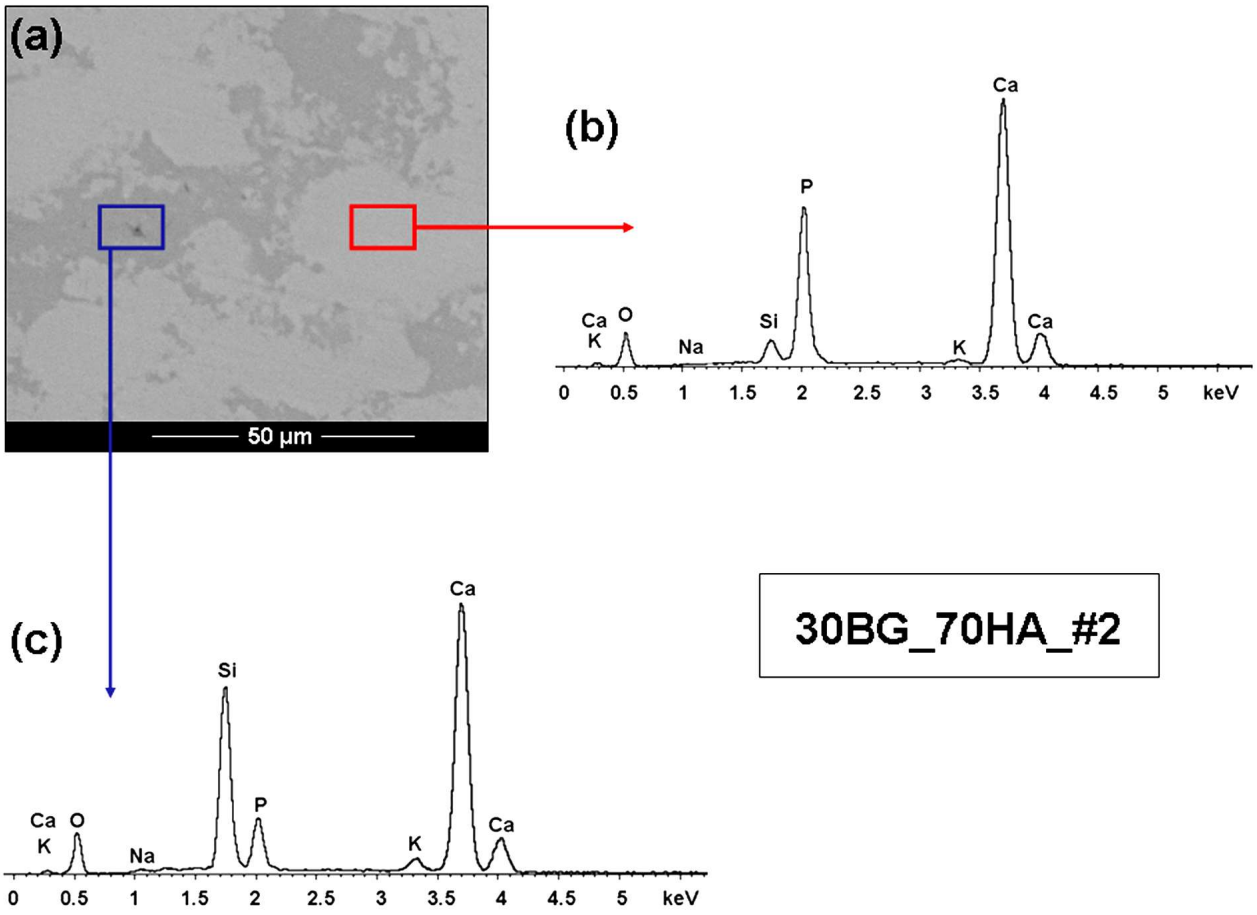

Figure 9. Micrograph of the 80BG_20HA#1 surface after 7 days in SBF (a) and results of the X-EDS analysis (b, c) performed on the areas indicated in (a).

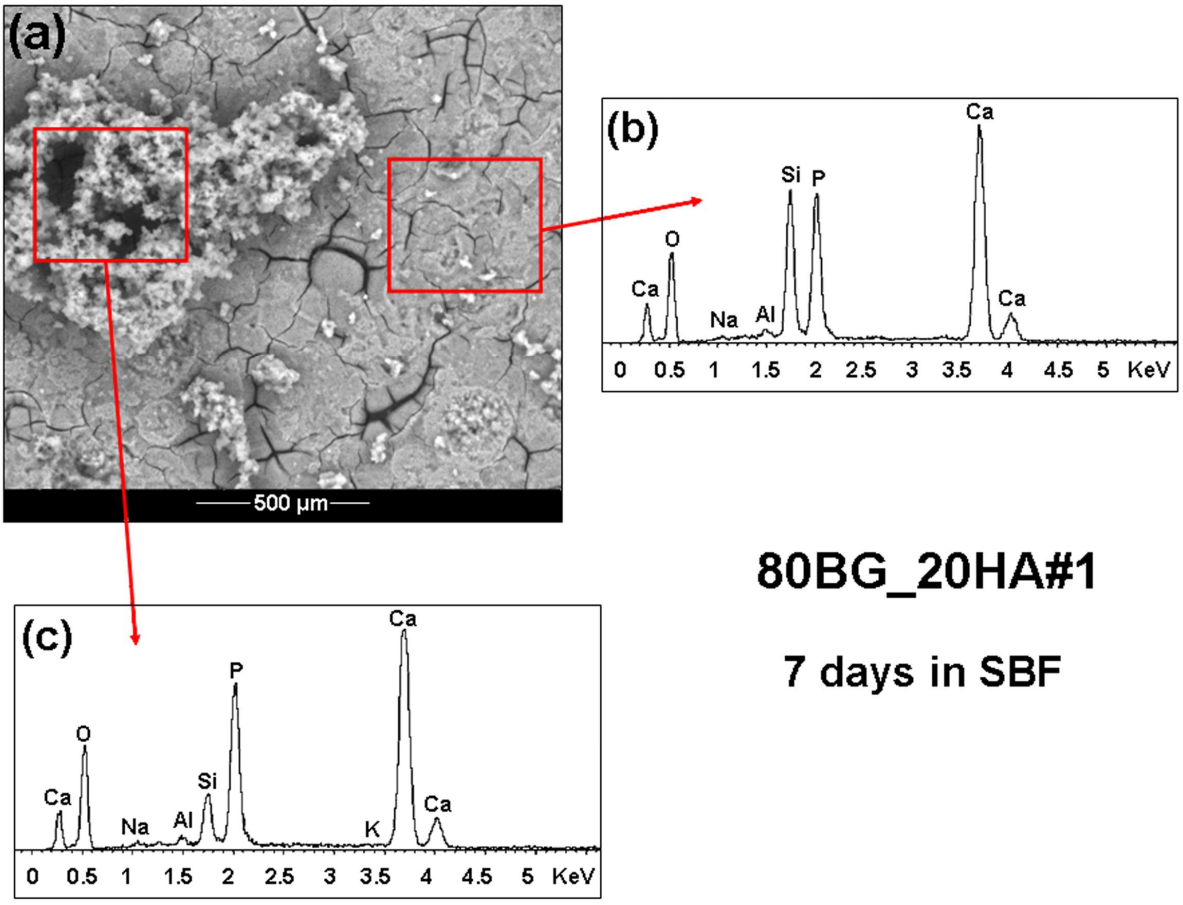

Figure 10. Micrograph of the 80BG_20HA#1 surface after 14 days in SBF.

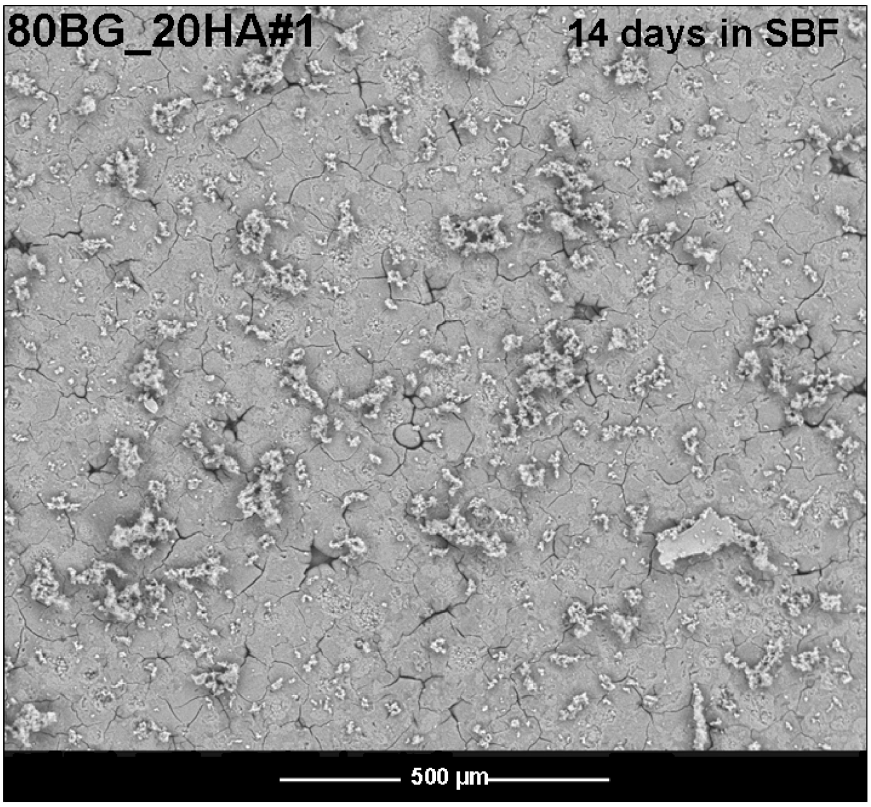

Figure 11. Raman spectra acquired on the precipitates formed on the 80BG_20HA#1 surface after 14 days in SBF.

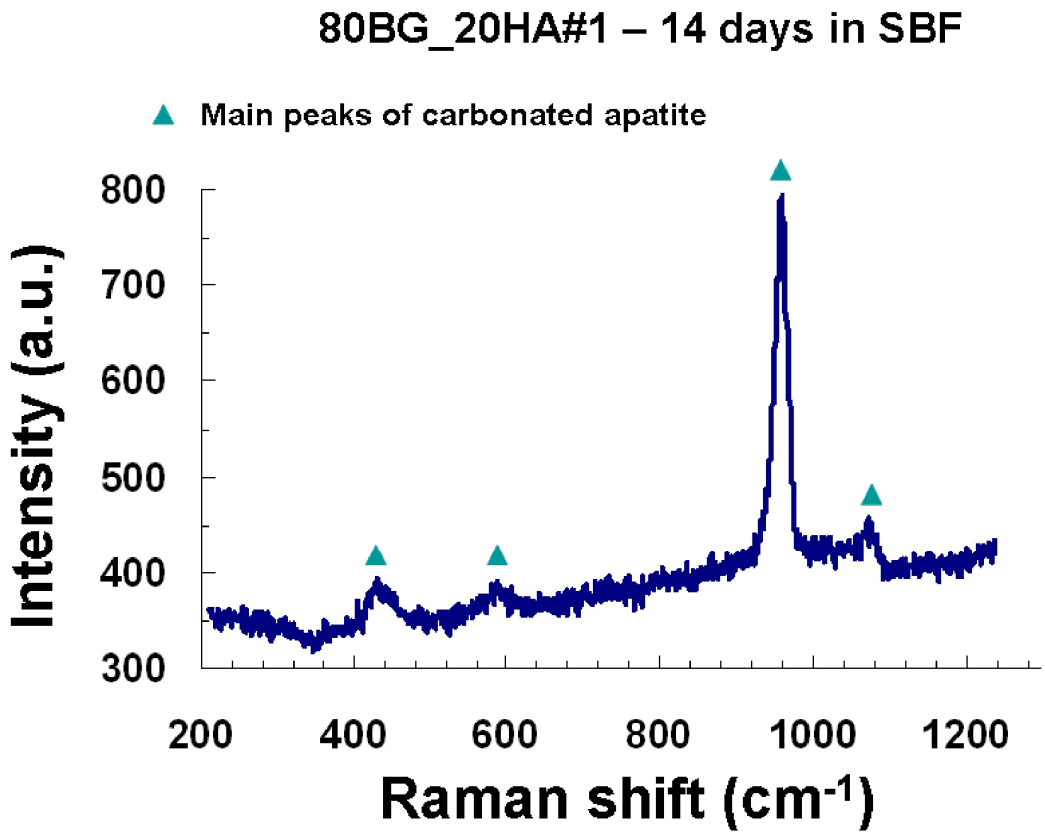

Figure 12. SEM images of the SPSed HA (a), 30BG_70HA#1 (b), 50BG_50HA (c) and 80BG_20HA#1 (d) samples after 3 days in SBF.